Chapter 4
Introduction to Evaporative Heat Transfer

Manish Bhendura, K. Muralidhar, and Sameer Khandekar

Nomenclature

a	Coefficient of velocity distribution function
c_{pa}	Specific heat capacity of air at constant pressure (J/kg K)
D	Mass diffusivity of water vapor in dry air (m^2/s)
f_M	Maxwellian velocity distribution function
F	Correction factor for total mass flux
G	Correction factor for total y-momentum flux
g	Gravitational acceleration (m/s^2)
h_c	Convective heat transfer coefficient (W/m^2 K)
h_e	Evaporative heat transfer coefficients (W/m^2 K)
h_{fg}	Latent heat of vaporization of water (J/kg)
H	Correction factor for total energy flux
j	Molecular evaporative mass flux in kinetic model (kg/m^2 s)
k_B	Boltzmann's constant (J/K)
k_m	Thermal conductivity of mth fluid (W/m K)
m_e	Evaporative mass flux of water in continuum model (kg/m^2 s)
M_a	Molecular mass of air (kg/kmol)
M_w	Molecular mass of water (kg/kmol)
n	Molecular density (mol/m^3)
p	Saturation pressure of water vapor at a given temperature (kPa)
p'	Partial vapor pressure of water in saline water (kPa)
p_T	Total pressure (kPa)
Q	Binary collision integral
q_e	Evaporative heat flux (W/m^2)
R	Gas constant of water vapor (J/kg K)
S	Dimensionless speed ratio

t	Time (s)
T	Temperature (K); suffix c and w for cold and water surface
u	Speed of bulk flow (m/s)
u_m	Tangential velocity component of mth fluid (m/s)
v_m	Velocity vector of mth fluid (m/s)
X_w	Mole fraction of water in the salt solution
y	Directional length normal to the liquid-vapor interface (m); continuum model
Z	Pressure ratio

Greek Letters

α	Accommodation coefficient of water evaporation
α_c	Condensation coefficient
α_e	Evaporation coefficient
α_m	Thermal diffusivity of mth fluid (m^2/s)
β_m	Thermal expansion coefficient of mth fluid (K^{-1})
γ	Unit vector directed vertically upward
ξ_y	y-component (normal) of molecular velocity vector (m/s)
θ	Temperature ratio
μ_m	Dynamic viscosity of mth fluid (Pa s)
ν_m	Kinetic viscosity of mth fluid (m^2/s)
ξ	Molecular velocity vector (m/s)
ρ_m	Density of mth fluid (kg/m^3)
ψ	Arbitrary function for total fluxes of mass, y-momentum, and energy
ω	Absolute humidity of air

Subscripts and Superscripts

∞	Vapor side in kinetic model
0	Liquid side in kinetic model
e	Emitted
r	Reflected
+	Outward flux
−	Inward flux

4.1 Introduction

Evaporation is a spontaneous liquid-to-vapor phase change process, seen in a variety of contexts including the natural hydrological cycle of earth. It serves as a natural thermal control mechanism of living and breathing animals. In the process industry, evaporation is an important intermediate step in drying operations and in water

purification via distillation. Low temperature applications of evaporation can be seen in devices providing indoor thermal comfort while evaporation of thin films has been proposed as an effective technique for thermal management of intense heat generating devices such as those in miniature electronics.

Evaporation is a heterogeneous phase change phenomenon, in which a surface molecule of matter in the low energy liquid state jumps to a high energy vapor state. The energy transition is accompanied by the transfer of latent heat of vaporization from adjacent molecules, causing a thermal perturbation at the liquid-vapor interface. The transfer of latent heat from the molecule in the liquid phase to the vapor is isothermal but will tend to cool the liquid body. The molecule that has passed into the vapor phase has definite kinetic energy and will diffuse into its surroundings, thus initiating vapor phase mass transport. Evaporation of a liquid body into a gas phase (air, in the present discussion) is spontaneous if the gas phase above is dry, relative to saturation conditions, defined by the prevailing pressure and temperature. Therefore, evaporation involves heat transfer in the liquid phase and simultaneous heat and mass transport in the vapor phase, with the liquid-vapor interface serving as a thermally active boundary.

In the simplest form, evaporation is considered a multiscale, multiphase, and multiphysics phenomenon. The scales arise from the gas and liquid phases, apart from molecular scales of diffusion and larger scales of fluid convection. In terms of distinct physical processes, we have heat transfer in the individual phases coupled at the interface, mass transfer of moisture across the interface and within the gaseous region, possible transport of solutes within the liquid body as well as buoyant- and Marangoni-driven flow in the liquid body. These processes are intrinsically coupled and require an elaborate mathematical model for analysis. In device modeling, for example, solar stills, evaporation is represented empirically in terms of an evaporative mass flux stated in terms of a sink temperature and the temperature of the evaporating liquid surface. Such models need to be validated against a full experiment backed by detailed numerical simulation.

4.2 Evaporation Models

These are broadly divided into two categories depending on the treatment of the air-water interface, as shown in Fig. 4.1. In a continuum model, interface temperature is continuous across the liquid and gas phases and is referred to as quasi-equilibrium (or, a local equilibrium) model, while variations in temperature, pressure, velocity, and other properties are permitted elsewhere in the fluid domain. Consideration of temperature jump at the interface originating from microscale processes constitutes the non-equilibrium model. Models arising from these two criteria are discussed here.
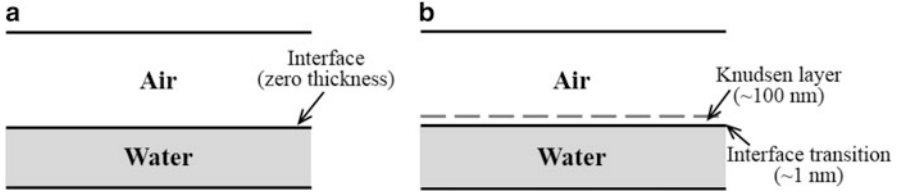
Fig. 4.1 (**a**) Air-water interface assumed to be in quasi-equilibrium with each of the phases; (**b**) non-equilibrium conditions revealed the appearance of a Knudsen layer

4.2.1 Quasi-Equilibrium Model

In a quasi-equilibrium model, temperature varies continuously from the liquid side to the gas side, while the jump in heat flux at the liquid-gas interface is fully accounted for in terms of the latent heat absorbed. Specifically, temperature jump is zero at the interface. Model statement developed under this framework in the form of differential equations is presented below.

Following evaporation, water vapor diffuses in the surrounding air and towards a region of lower humidity. Water vapor is transported in air and sets up a moisture concentration field. The gradient of moisture concentration at the air-water interface controls the evaporation rate. One can now state a species transport equation for moisture in the gas phase. In applications where the air-water interface is practically stationary, transport of water vapor by evaporation may be taken as diffusion dominated and the mass flux of water vapor (kg/m^2-s) calculated using the Fick's law

$$\dot{m}_e = -\rho_a D \frac{\partial \omega}{\partial y} \tag{4.1}$$

Here, ω is the absolute humidity of air (kg vapor/kg of dry air), ρ_a is the density of dry air (kg/m^3), and D is mass diffusivity of water vapor in dry air (m^2/s). The corresponding evaporative heat flux (W/m^2) at the interface is the product of evaporation rate and the latent heat of vaporization (J/kg), namely

$$\dot{q}_e = \dot{m}_e h_{fg} \tag{4.2}$$

To obtain the evaporation rate using Eq. (4.1), the moisture field must be known in the surrounding air. This distribution can be determined by solving an advection-diffusion equation for humidity along with suitable initial and boundary conditions.

In a simplified quasi-equilibrium model (Tiwari and Sahota 2017), an evaporative heat transfer coefficient is empirically specified to estimate the evaporative heat flux, and in turn, the evaporation rate. For a body of warm water evaporation into a cold surface, this prescription is

$$\dot{q}_e = h_e(T_w - T_c) \tag{4.3}$$

Here, q_e and h_e are the evaporative heat flux and evaporative heat transfer coefficient, respectively, and T_w and T_c are the temperature of water surface and the average cold surface temperature, respectively. The evaporative heat transfer coefficient can be connected to the convective heat transfer coefficient (h_c) using the definitions of partial pressures (p_w, p_c) and humidity ratio

$$\frac{h_e}{h_c} = \left(\frac{h_{fg}}{c_{pa}}\right)\left(\frac{M_w}{M_a}\right)\left(\frac{p_w - p_c}{T_w - T_c}\right)\left(\frac{p_T}{(p_T - p_w)(p_T - p_c)}\right) \tag{4.4}$$

Here, h_{fg} is the latent heat of vaporization of water (J/kg), c_{pa} is the specific heat of air (J/kg K), M_w and M_a are the molecular masses of water and air, respectively, and p_T is the total pressure. Equation (4.4) is quite useful for the estimation of the evaporative heat transfer coefficient since correlations are available in the literature for the convective heat transfer coefficient. Dunkle's correlation is one of these and is derived for non-isothermal convection in an air-water system inside an enclosure. It is expressed as

$$h_c = 0.844\left[(T_w - T_c) + \frac{(p_w - p_c)T_w}{(268.9 - p_w)}\right]^{\frac{1}{3}} \tag{4.5}$$

Here, T_w and T_c are the bulk temperature of water and average temperature of the cold surface, respectively. Pressures are expressed in units of kPa and temperature in Kelvin.

The quasi-equilibrium model with a correlation for the interfacial heat transfer coefficient is extensively used in the analysis of solar distillation systems. Here, the liquid body comprises saline water and the condensate is potable water. Salinity affects the evaporation rate of water since it regulates the saturation pressure for a given temperature. This change in saturation pressure is accounted for by Raoult's law, which states that the vapor pressure of a solvent (water) in a solution (saline water) is

$$p'_w = X_w p_w \tag{4.6}$$

Here, X_w is the mole fraction of water in the salt solution and is less than unity. Thus, the effect of salt in water is to diminish the saturation pressure and thus lower evaporation rates. Vapor pressure depression can be explained in terms of the reduction of chemical potential of water due to an increase in the salt ion activity. The influence is more pronounced at higher temperatures since the ionic activity is also elevated (Kokya and Kokya 2008).

4.2.2 Transport Equations in a Two-Layer Air-Water System

In water purification applications, water is heated by an external agency, while the surrounding air is cooled externally using an active cold surface to increase the evaporation rate and maximize condensation of pure water. A negative temperature gradient is set up in both air and water, which results in two-layer natural convection. The gradient in humidity is opposed to gravity and can stabilize convection in air. Heat transfer rates in air and water influence interfacial temperature, which, in turn, affects the evaporation rate. Hence, the device performance depends on transport phenomena at all scales of transport prevailing in the cavity.

The complete transport model of evaporation with associated initial and boundary conditions are laid out in this section for a rectangular cavity that is partially filled with water, the rest being air. The water body is taken to be initially warm; the top surface is cold, other surfaces are insulated, and air is initially dry. Evaporation from the air-water interface consumes the latent heat of evaporation from the water body that progressively cools with time. The temperature differential in water is gravitationally unstable and generates buoyancy-driven convection. Surface tension gradients over the gas-liquid interface may generate additional convection as well. From thermal considerations alone, density gradient in air is unstable and heat transfer would be controlled by buoyant convection. The interface region contains practically moisture-saturated air while it is relatively dry at the cooler surface where water has condensed. Hence, a gravitationally stable density gradient may form in air and the resulting strength of convection currents will respond to the difference between the body forces related to the heat and mass transfer mechanisms.

A rectangular enclosure partially filled with initially hot water is considered for the formulation of transport models in air and water, Fig. 4.2. Governing equations applicable for a two-dimensional geometry are written out in the following discussion. Flow is taken to be unsteady but laminar; buoyancy is included but surface tension gradients are neglected. The two phases are clearly separated across an interface. The air-water interface is always flat and horizontal; change in water level with time is neglected though it can be easily accounted for. Water condensing at the top cooled wall is assumed to be drained away immediately so that a single-

Fig. 4.2 Schematic of a rectangular enclosure, thermally insulated from all sides except the top and partially filled with initially hot water
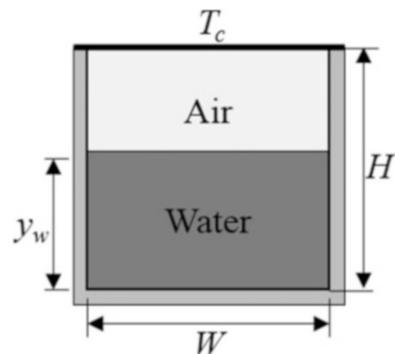
phase model of transport in air is applicable here. The gradient in temperature within the cavity will be responsible for Rayleigh-Benard convection that is intrinsically three dimensional. The two-dimensional treatment may correspond to an average temperature field determined with respect to the dimension along the length of the cavity.

The mass, momentum, and energy balance equations for air and water are as follows (Nepomnyashchy and Simanovskii 2004):

$$\nabla \cdot \vec{v}_m = 0 \tag{4.7}$$

$$\frac{\partial \vec{v}_m}{\partial t} + \left(\vec{v}_m \cdot \nabla\right)\vec{v}_m = -\frac{1}{\rho_m}\nabla p_m + \upsilon_m \nabla^2 \vec{v}_m - g[1 - \beta_m(T_m - T_c)]\hat{\gamma} \tag{4.8}$$

$$\frac{\partial T_m}{\partial t} + \vec{v}_m \cdot \nabla T_m = \alpha_m \nabla^2 T_m \tag{4.9}$$

Here, index m is used to denote the two fluids; $m = 1$ is water, while 2 is air. Quantities $\vec{v}_m, p_m,$ and T_m are the velocity vector, pressure, and temperature fields of the mth fluid. Additionally, $\rho_m, \upsilon_m, \beta_m,$ and α_m are the density, kinetic viscosity, thermal expansion coefficient, and thermal diffusivity of the respective fluid, while $\hat{\gamma}$ is a unit vector directed vertically upward.

Initially $(t = 0)$, water inside the enclosure is hot $(T_1 = T_h)$ and filled up to a depth of y_w, while air above is at the cold temperature $(T_2 = T_c)$. In most applications, the cold temperature is the ambient value. The fluid phases are both initially stagnant $\left(\vec{v}_m\,(t = 0) = 0\right)$.

The two vertical side walls and the lower surface are insulated. Hence, $\hat{n} \cdot \nabla T_m = 0$, whereas the top surface is maintained at the cold temperature. All four walls enforce the no-slip boundary condition, $\vec{v}_m = 0$. At the air-water interface, tangential and normal velocity components are continuous, shear stresses are continuous, and phase heat fluxes are separated by the latent heat release. In addition, the flatness of the interface condition requires the normal velocity component to be zero. Symbolically, these interface conditions are expressed as

$$\mu_1 \frac{\partial u_1}{\partial y} = \mu_2 \frac{\partial u_2}{\partial y} \quad \text{and} \quad u_1 = u_2; \quad v_1 = v_2 = 0 \tag{4.10}$$

$$-k_1 \frac{\partial T_1}{\partial y} = -k_2 \frac{\partial T_2}{\partial y} + q_e \quad \text{and} \quad T_1 = T_2 \tag{4.11}$$

where μ_m and k_m are the dynamic viscosity and thermal conductivity of the mth fluid. The evaporative heat flux q_e is estimated by utilizing one of the evaporation models described earlier, via a correlation (via Eq. (4.3) with the correlation Eq. (4.4)) or via the gradient of humidity (specifically, the evaporation rate) multiplied by the latent heat of vaporization (Eqs. 4.1 and 4.2).

Computation of the humidity gradient requires the solution of the moisture transport equation in air. The governing equation for moisture transport in air is of the advection-diffusion type

$$\frac{\partial \omega}{\partial t} + \vec{v}_2 \cdot \nabla \omega = D \nabla^2 \omega \tag{4.12}$$

where ω is the absolute humidity of air, and D is the mass diffusivity of water vapor into air.

The binary mass diffusivity of air and water vapor, D is the strong function of temperature and pressure, which can be estimated using the following expression (Bird et al. 2002):

$$D = a \frac{T^b}{p} \tag{4.13}$$

Here, D is in m^2/s, p in atm, and T in K and the constants are $a = 0.434 \times 10^{-10}$ and $b = 2.334$. A typical value of the binary mass diffusivity is 2.5×10^{-5} m^2/s.

Air is initially assumed to be dry, i.e., $\omega = 0$ (or partially saturated), whereas at the interface and at the top surface, air is saturated with water vapor at the local temperature; in other words, the value of ω is specified at these boundaries. The moisture content under saturation conditions is calculated using

$$\omega_s = \frac{M_a}{M_w} \times \frac{p_s}{p_T - p_s} \tag{4.14}$$

where M_a and M_w are the molecular masses of the air and water, respectively, and p_s and p_T denote the saturation pressure and total pressure (in Pa), respectively. The saturation pressure of water can be calculated using empirical relations proposed by numerous researchers. The correlation used in the design of solar distillation systems is

$$p_s(T) = \exp\left(25.317 - \frac{5144}{T}\right) \tag{4.15}$$

where T is in units of Kelvin and pressure is recovered in Pa.

The governing equations of phase velocity, pressure, temperature, and humidity are clearly nonlinear and coupled. These can only be solved numerically using sophisticated computational tools.

4.2.3 Non-Equilibrium Model

We present here a simplified form of the non-equilibrium model by neglecting the presence of air. Air is treated as a non-condensable gas and significantly alters the evaporation rate. Specifically, the evaporation rate in humid air is smaller than in pure vapor for a given temperature difference. For equal evaporation rates, humid air would require a higher temperature difference when compared to pure vapor. In addition, evaporation in humid air will give rise to a diffusion layer that is rich in vapor. This contrasts with condensation of vapor from moist air, where the diffusion layer is rich in air. These corrections can be determined from kinetic theory of gases but is beyond the scope of the present discussion.

In the non-equilibrium model of a liquid-vapor system, two microscopic layers appear between the bulk phases of water and vapor—the interface transition layer and the Knudsen layer (Fig. 4.3). The interface transition thickness is of few molecular diameters (~0.25–1 nm), across which the liquid density transitions to vapor density. Evaporation causes a small but a nearly discontinuous temperature jump in this layer. The thickness of this layer may be approximated as zero and considered to be a part of the liquid surface.

The Knudsen layer is located between the interface transition layer and the bulk vapor phase. Its thickness is of the order of a few free molecular mean-free paths (~10–150 nm). It involves interaction among molecules arising from three sources. These are molecules emerging from the liquid surface, molecules impinging on the liquid surface from the vapor side and molecules of the vapor phase reflected from the liquid surface. The molecules are indistinguishable and do not represent any chemical reaction. A net positive molecular flux at the outer boundary of the Knudsen layer results in evaporation. A negative flux of molecules ensures condensation. In case of zero net flux, the liquid-vapor system around the interface is taken to be in thermal, mechanical, and chemical equilibrium.

Molecular interaction in thin regions such as the Knudsen layer can result in large temperature changes and hence alter heat and flow characteristics of bulk phases involved in phase change. However, first principles modeling of transport in the Knudsen layer is difficult since continuum principles of density, pressure, and

Fig. 4.3 Schematic representation of temperature drop along the interface transition layer $(T_1 - T_0)$ and the Knudsen layer $(T_0 - T_\infty)$
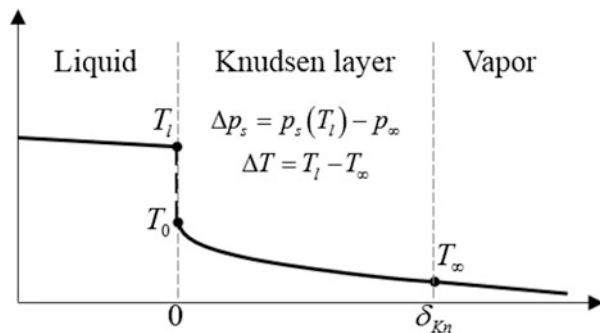
temperature are not applicable (Gerasimov and Yurin 2018). An alternative is a molecular approach, for example, the molecular kinetic theory (MKT) that can determine changes in the macroscopic quantities due to molecular interaction in a gap of a few molecular mean-free paths.

4.2.4   Kinetic Theory of Gases

The molecular kinetic theory involves the velocity distribution function for molecules in a probabilistic context. In a collection of particles moving in time and space with a wide spread of velocities, the distribution function represents the fraction of molecules in a specified velocity interval. The commonly used Maxwell's distribution function is an example of such a variation but holds only under conditions of thermodynamic equilibrium. Vapor molecules leaving the liquid surface into the Knudsen layer will generally show departure from equilibrium and the distribution function will deviate from the Maxwellian. Differences are expected to be large at temperatures closer to the boiling point of the liquid. The molecular velocity distribution function, once found by other methods, can be utilized to estimate macroscopic parameters such as number density, bulk velocity, and temperature, including the temperature jump. The molecular interactions inside the Knudsen layer can be analyzed using the transport equation of velocity distribution function and is known as the Boltzmann's kinetic equation (BKE).

For closure of BKE, boundary conditions for the Knudsen layer at the inlet (towards the transition layer) and the outlet (towards the vapor bulk phase) are required. The inlet velocity distribution function depends on the molecule emission rate from the transition layer. It can be predicted reasonably well by molecular dynamic simulations (MDS). The outlet boundary condition (velocity distribution) is defined at the thermodynamic state of the bulk vapor phase. Hence, the solution of MDS is the boundary condition for BKE, whereas the solution of BKE is utilized as the boundary condition for the continuum analysis of the bulk phases (Shishkova et al. 2017).

The involvement of two statistical approaches (MDS and MKT) results in a comprehensive but difficult and computationally expensive methodology. The complexity can be reduced by avoiding MDS and using an approximate velocity distribution function at the inlet boundary of the Knudsen layer (Frezzotti et al. 2018). The half-space Maxwellian distribution is one such distribution well-known in the kinetic theory of evaporation and has been utilized in the following discussion. Under this simplification, evaporation mass flux can be estimated though tempertaure jump and the thickness of the Knudsen layer are no longer be resolved.

The evaporation models based on the molecular kinetic theory are further discussed below (Aursand and Ytrehus 2019).

Using the kinetic theory of gases approach, the velocities of molecules are denoted probabilistically by the Maxwell velocity distribution. The probability

density function of velocity represents the fraction of the total number of molecules at a given point (x, t) having velocities in a specific range is

$$f_M(\xi; T, n, u) = \frac{n}{(2\pi RT)^{3/2}} \exp\left(-\frac{(\xi - u\widehat{y})^2}{2RT}\right) \tag{4.16}$$

Here, x is position vector, t is time, ξ is a molecular velocity vector, n is number density of elementary particles, and u is the speed of bulk flow along the y-axis. This distribution is further utilized to compute the fluxes of mass, y-momentum, and kinetic energy of molecules evaporating from the interface into the Knudsen layer. The outgoing particles ($\xi > 0$) from the liquid surface are postulated to be half of the Maxwellian distribution corresponding to the reference state. Total fluxes of mass, y-component momentum, and kinetic energy of a molecule are expressed in terms of the Maxwellian distribution. A function ψ_i ($i = 1$, 2, and 3) is defined to represent these fluxes

$$\psi_i = (m, m\xi_y, \frac{1}{2}m\xi^2) \tag{4.17}$$

Hence, the net outgoing fluxes ($y > 0$) are

$$\int_{\xi > 0} \xi_y \psi_i f_M \mathrm{d}\xi = \begin{cases} \rho\sqrt{\dfrac{RT}{2\pi}}F^+(S), & i = 1 \\[2mm] \rho\dfrac{RT}{2}G^+(S), & i = 2 \\[2mm] 2\rho RT\sqrt{\dfrac{RT}{2\pi}}H^+(S), & i = 3 \end{cases} \tag{4.18}$$

The net inward fluxes ($y < 0$) are

$$\int_{\xi < 0} \xi_y \psi_i f_M \mathrm{d}\xi = \begin{cases} -\rho\sqrt{\dfrac{RT}{2\pi}}F^-(S), & i = 1 \\[2mm] \rho\dfrac{RT}{2}G^-(S), & i = 2 \\[2mm] -2\rho RT\sqrt{\dfrac{RT}{2\pi}}H^-(S), & i = 3 \end{cases} \tag{4.19}$$

where $F^\pm(S)$, $G^\pm(S)$, and $H^\pm(S)$ are correction factors to include the effect of bulk molecular flow; these functions are defined

$$F^\pm(S) = \sqrt{\pi}S(\mathrm{erf}(S) \pm 1) + \mathrm{e}^{-S^2} \tag{4.20}$$

$$G^{\pm}(S) = (2S^2 + 1)(\text{erf}(S) \pm 1) \pm \frac{2}{\sqrt{\pi}} e^{-S^2} \tag{4.21}$$

$$H^{\pm}(S) = \frac{\sqrt{\pi}S}{2}\left(S^2 + \frac{5}{2}\right)(\text{erf}(S) \pm 1) + \frac{1}{2}(S^2 + 2)e^{-S^2} \tag{4.22}$$

The dimensionless speed ratio (S) is

$$S(u, T) = \frac{u}{\sqrt{2RT}} \tag{4.23}$$

The three correction factors approach unity, when S is small.

In the calculation of the evaporative mass flux, a collision-free transport of molecules through the Knudsen layer under a high-vacuum condition is assumed for each of its boundaries. The net mass flux at a boundary is the difference between the incoming molecules and outgoing molecules. The two boundaries of the Knudsen layer are at temperatures T_1 (liquid side) and T_∞ (vapor side). Bulk flow of the vapor molecules is not considered in the present formulation ($u = 0$). Therefore, the distribution of molecules emerging from the liquid surface is

$$f_e = f_M(\xi; T_1, n_e, u = 0) \tag{4.24}$$

The distribution of molecules coming out of the vapor side towards the liquid boundary is

$$f_\infty = f_M(\xi; T_\infty, n_\infty, u = 0) \tag{4.25}$$

The resulting evaporation flux is derived as

$$j = \alpha[\int_{\xi>0} \xi_y \psi_1 f_e d\xi + \int_{\xi<0} \xi_y \psi_1 f_\infty d\xi] \tag{4.26}$$

$$= \alpha\left[\frac{p_s(T_1)}{\sqrt{2\pi RT_1}} - \frac{p_\infty}{\sqrt{2\pi RT_\infty}}\right] \tag{4.27}$$

where α is a pre-factor, known as the accommodation coefficient of evaporation, falling in the range of 0 to 1. It is connected to the extent to which molecules originating from the vapor side are reflected at the vapor-liquid interface.

In Eq. (4.27), temperature T_∞ (the vapor side temperature) is unknown and must be the outcome of the evaporation model. In order to improve the utility of Eq. (4.27), an ad hoc assumption is often implemented. The assumption states that the vapor at the outer boundary of the Knudsen layer is fully saturated, namely

$$T_\infty = T_s(p_\infty) \tag{4.28}$$

For weak evaporation, the temperature difference across the Knudsen layer is small and the evaporation flux is further reduced to the Hertz-Knudsen (HK) formula

$$j = \alpha \left[1 - \frac{1}{2} \frac{RT_1}{h_{\text{fg}}} \right] \frac{\Delta p_{\text{s}}}{\sqrt{2\pi RT_1}} \tag{4.29}$$

where, as before, h_{fg} is the latent heat of vaporization, and $\Delta p_{\text{s}} = p_{\text{s}}(T_1) - p_{\infty}(T_{\text{s}})$.

An improvement over the Hertz-Knudsen formula was made by including the effect of bulk vapor molecular flow in the formulation. The outgoing Maxwellian distribution for the vapor side boundary is written

$$f_{\infty} = f_{\text{M}}(\xi; T_{\infty}, n_{\infty}, u_{\infty}) \tag{4.30}$$

The resulting evaporation flux, known as the Schrage-Mills (SM) formula is

$$j = \alpha \left[\frac{p_{\text{s}}(T_1)}{\sqrt{2\pi RT_1}} - \frac{p_{\infty}}{\sqrt{2\pi RT_{\infty}}} F^-(S_{\infty}) \right] \tag{4.31}$$

The bulk velocity correction factor $F^-(S_{\infty})$ is calculated using Eq. (4.20) with dimensionless speed ratio evaluated at temperature T_{∞}. The temperature T_{∞} is again an unknown and the difficulty is accounted for using the assumption of Eq. (4.28).

Equation (4.31) reduces for weak evaporation ($S_{\infty} \ll 1$) to

$$j = \frac{\alpha}{1 - 0.5\alpha} \left[1 - \frac{1}{2} \frac{RT_1}{h_{\text{fg}}} \right] \frac{\Delta p_{\text{s}}}{\sqrt{2\pi RT_1}} \tag{4.32}$$

In the Boltzmann Equation Moment Method (BEMM) model, the y-momentum and energy conservation equations across the Knudsen layer are included, contrary to the earlier formulations. Accordingly, the model predicts the vapor side boundary temperature (T_{∞}) as well. Three conservation equations are solved for the Knudsen layer using the one-dimensional, steady-state version of the Boltzmann equation

$$\xi_y \frac{\partial f}{\partial y} = Q(ff_1) \tag{4.33}$$

Equation (4.33) is an integro-differential equation for the y-velocity component with the binary collision integral (Q) on the right-hand side. It is the rate of change of the distribution function f during collision with another particle with a partner distribution function f_1 (Ytrehus and Østmo 1996).

The Knudsen layer consists of three probabilistic velocity distributions at its two boundaries: the outgoing distribution ($f^+(0, \xi)$) at the liquid side boundary ($y = 0$); the incoming distribution ($f^-(\infty, \xi)$) and the outgoing ($f^+(\infty, \xi)$) distribution on the vapor side boundary ($y \to \infty$). The following forms of the three distributions as boundary conditions for Eq. (4.33) facilitate a closed-form solution:

$$f(y, \xi) = a_0^+(y)f^+(0, \xi) + a_\infty^+(y)f^+(\infty, \xi) + a_\infty^-(y)f^-(\infty, \xi) \qquad (4.34)$$

The y-dependent coefficient a's have boundary conditions

$$\text{At } y = 0 \quad a_0^+ = 1 \quad a_\infty^+ = 0 \quad a_\infty^- = \beta$$
$$\text{At } y = \infty \quad a_0^+ = 0 \quad a_\infty^+ = 1 \quad a_\infty^- = 1$$

Using these conditions with Eq. (4.34), the probability distribution for velocity on the vapor side boundary can be written as

$$f(\infty, \xi) = f^+(\infty, \xi) + f^-(\infty, \xi) \qquad (4.35)$$

This distribution may be taken as prevailing in the bulk vapor state. Similarly, the outgoing velocity distribution for the liquid surface can be written as

$$f(0, \xi) = f^+(0, \xi) + \beta f^-(\infty, \xi) \qquad (4.36)$$

where the symbol β is an unknown parameter related to the incoming velocity distribution at the outer boundary of the Knudsen layer ($y \to \infty$). The outgoing distribution at the liquid surface can further be divided into an emission part and a reflection part

$$f^+(0, \xi) = \alpha_e f_e^+(0, \xi) + (1 - \alpha_c)f_r^+(0, \xi) \qquad (4.37)$$

where α_e and α_c are the evaporation-coefficient and condensation-coefficient, respectively. Functions $f_e^+(0, \xi)$ and $f_r^+(0, \xi)$ are the emission and reflection distributions, respectively. These distributions are assumed to be Maxwellian (Eq. 4.16) at the liquid temperature, but with a number densities n_e and n_r, respectively.

The number density n_r in the reflection distribution is estimated by equating the incoming flux on the vapor side boundary to the reflected flux on the liquid side boundary

$$\frac{n_r}{n_\infty} = \beta\sqrt{\frac{T_\infty}{T_l}}F^-(S_\infty) \qquad (4.38)$$

The boundary condition at $y = 0$, can be written as

$$f(0, \xi) = \begin{cases} \left(\alpha_e + (1 - \alpha_c)\dfrac{n_r}{n_e}\right)f_e^+(0, \infty) & \xi_y > 0 \\ \beta f_\infty^- & \xi_y < 0 \end{cases} \qquad (4.39)$$

Equation (4.33) of the kinetic theory model is solved next with the boundary conditions (Eqs. 4.35 and 4.39). The input variables are the properties of the bulk

liquid surface (T_l) and corresponding number density $n_e(=\rho_l/(k_BT_l))$ and the outputs of the model are the properties of the bulk vapor phase, T_∞, u_∞, and β.

These equations are solved using the moment method, in which the mass, y-momentum, and energy are stated to be collision-invariants. This statement is expected to be valid for the kinetic theory model when it is solved for the outer boundary parameters (T_∞ and u_∞) of the Knudsen layer, instead of a full solution in the entire vapor phase. The approximation eliminates the need of a collision model, namely function $Q(ff_1)$. Thereafter, the moment equations are generated using the function ψ_i defined in Eq. (4.17). The basic form of moment equations is expressed as

$$\frac{\partial}{\partial y} \int \psi_i(\xi)\xi_y f(y,\xi)\,\mathrm{d}\xi = 0 \quad (i = 1, 2, 3) \tag{4.40}$$

These integrals can be split into an outgoing part ($y > 0$) and incoming part ($y < 0$), which are further evaluated for the half Maxwellian distribution (Eq. 4.16) using Eqs. (4.18) and (4.19). This formulation leads to three conservation equation for mass, momentum, and energy in non-dimensional form, with four dependent variables ($S_\infty, \mathbb{Z}, \theta,$ and β). Among these, parameters $S_\infty, \mathbb{Z},$ and θ are the dimensionless speed ratio $\left(u_\infty/\sqrt{2RT_\infty}\right)$, pressure ratio ($p_s(T_l)/p_\infty$), and temperature ratio (T_∞/T_l), respectively. These equations are solved by specifying one of the unknown variables and solving for the other three parameters. Based on these values, the evaporative mass flux can finally be calculated

$$j = \frac{p_\infty}{RT_\infty} u_\infty; q = j \times h_{fg} \tag{4.41}$$

In case a known pressure (p_∞ or $\mathbb{Z}$) boundary condition is imposed outside the Knudsen layer, Eq. (4.41) can be reduced to

$$j = \frac{p_\infty}{\sqrt{RT_l}} \sqrt{\frac{2}{\theta}} S_\infty \tag{4.42}$$

The kinetic theory models are likely to be accurate since they account for the temperature jump across the air-water interface. Among the kinetic theory models, the BEMM model is preferable under strong evaporation conditions, while SM should be comparable to BEMM for weak evaporation (Aursand and Ytrehus 2019).

Polikarpov et al. (2019) compared the experimental data of Badam et al. (2007) and Kazemi et al. (2017) on interfacial evaporation rate and temperature jump to the available SM and BKE-based non-equilibrium models. The SM formula overestimated the evaporation rate whereas the BKE-based kinetic model predicted the evaporation rate reasonably well. The interfacial temperature jump from BKE did not show good agreement with experiments.

The evaporative mass flux obtained from the molecular kinetic theory can also be used as an interfacial boundary condition in the quasi-equilibrium model (Qin and Grigoriev 2015). In this approach, the transport equations (Eqs. 4.7–4.11) are solved with evaporative heat flux calculated from Eq. (4.2). The evaporation rate in this formulation is approximated by using the SM formula (Eq. 4.32), instead of Eq. (4.1).

4.2.5 Accommodation Coefficient

The accommodation coefficient is a macroscopic measure of the actual (experimental) evaporation/condensation flux when compared with the estimated (theoretical) flux. In molecular terms, the accommodation coefficient of evaporation is the ratio of the molecular flux emitted from liquid surface and the molecular flux transferred to the vapor phase. Similarly, the accommodation coefficient of condensation is defined as the ratio of molecular flux absorbed by the liquid surface to the molecular flux impinging on it, the difference being reflected from the interface.

In the literature, these evaporation and condensation coefficients are assumed to be equal. A value of unity will indicate an equilibrium condition though evaporation and condensation are strongly non-equilibrium phenomena. Hence, a unit accommodation coefficient may be applicable only for weak evaporation (Kryokov and Levashov 2011). These coefficients, though less than unity, are treated to be constant, but are expected to show dependence on temperature, pressure, and contaminants spread over the interface (Marek and Straub 2001). Accommodation coefficient may also be estimated by comparing kinetic theory predictions of macroscopic quantities such as heat fluxes and water production rate with a fully continuum-scale model. In principle, the quantification of accommodation coefficients requires molecular dynamic simulation and is a topic of research.

4.3 Closure

The quasi-equilibrium model of evaporation utilizes continuum tools and is conceptually simple. However, the resulting mathematical problem is coupled and nonlinear and can only be solved using approximate computational tools. The non-equilibrium model based on the kinetic theory is rich in physics and postulates the appearance of a Knudsen layer at the air-water interface. The extent of jump across the Knudsen layer in continuum-scale properties such as temperature, pressure, and velocity are expected to be important for microscale device-level applications of evaporation and condensation. These calculations are formulated using the framework of kinetic theory of gases. The significance of such Knudsen layer at the liquid-vapor interface in engineering applications remains to be conclusively established.